

Use of a pulsed fibre laser as an excitation source for photoacoustic tomography.

Thomas J. Allen¹, Shaiful Alam², Edward Z. Zhang¹,
Jan G. Laufer¹, David J. Richardson², Paul C. Beard¹

¹ Dept. of Medical Physics & Bioengineering, University College London, London, WC1E 6BT, UK

² Optoelectronics Research Centre, University of Southampton, Southampton, SO17 1BJ, UK

ABSTRACT

The use of a pulsed fibre laser as an excitation source for photoacoustic tomography has been investigated. Fibre lasers have the advantage of being compact, robust and efficient compared to traditional excitation sources used for photoacoustic tomography (e.g. Q-switched Nd:YAG pumped OPO or dye systems). Their high pulse repetition frequencies and adjustable pulse duration, shape and duty cycle also enables a wide range of time and frequency domain excitation methods to be investigated. A 1060nm, 20W fibre laser was used to generate acoustic waves in a tissue mimicking phantom composed of blood filled tubes immersed in a 1% solution of intralipid ($\mu'_s=1\text{mm}^{-1}$). The laser was then combined with a Fabry Perot photoacoustic imaging system to obtain 3D images of a tissue mimicking phantom and an *in vivo* image of the vasculature of the palm of a volunteer. This study has demonstrated that pulsed fibre lasers have potential application as an excitation source for photoacoustic imaging of superficial blood vessels.

Keywords: Fibre lasers, photoacoustic tomography

1. INTRODUCTION

Biomedical photoacoustic imaging techniques are based upon the generation of broadband (tens of MHz) ultrasonic waves by the absorption of nanosecond pulses of laser light in tissues. By detecting these acoustic waves at different points on the tissue surface, an image of the spatial distribution of the absorbed optical energy distribution can be obtained [1,2]. When imaging in tomography mode, in which full field illumination is used, laser pulse energies of several mJ are required. Q-switched Nd:YAG pumped OPO, Ti:Sapphire or dye laser systems can meet this requirement as well as the need for nanosecond pulse durations in order to achieve efficient photoacoustic generation. They can also emit in a desirable wavelength range (600-1200nm) where biological tissue is relatively transparent in order to achieve acceptable penetration depth. However, these systems tend to be bulky, expensive, require regular maintenance and provide low pulse repetition frequencies (<50Hz) thus limiting the image frame rate. As a consequence, although widely used as laboratory tools, their practical biomedical application, particularly within a clinical environment, remains limited.

Fibre laser technology offers the prospect of developing a compact, reliable and efficient photoacoustic excitation source for clinical use. Fibre lasers can provide high pulse repetition frequencies to achieve rapid image acquisition as well as pulses on demand for the implementation of photoacoustic Doppler flowmetry techniques [3]. They can also provide adjustable pulse duration, shape and duty cycle thus enabling a wide range of time domain excitation schemes to be explored. For example, pseudo random code schemes can be used to implement wavelength multiplexing for spectroscopic imaging [4] and pulse shaping techniques can be exploited to mitigate frequency dependent acoustic attenuation and improve generation efficiency [5]. Fibre lasers have previously been used in optical resolution photoacoustic microscopy (OR-PAM) [6,7] where the high beam quality ($M^2<1.2$) of the fibre laser can be exploited to provide a near-diffraction limited focused spot on the surface of the tissue. This type of photoacoustic imaging has the advantage of providing images with very high lateral spatial resolution (<10 μm) using modest pulse energies of a few ten's of μJ . However, in contrast to the tomography mode, it can only provide a strictly limited penetration depth of up to 1mm due to the strong optical scattering exhibited by soft tissues [8].

In this study, a fibre laser is used for the first time to implement the tomography mode of photoacoustic imaging in which full field excitation is used. Section 2.1 describes single point measurements made in a tissue mimicking phantom

in order to evaluate SNR in the first instance. Sections 2.2 and 2.3 discuss the photoacoustic images obtained in tomography mode when imaging a tissue mimicking phantom and the vasculature of the palm of a volunteer, respectively.

2. METHOD & RESULTS

2.1 Single point measurements in a tissue mimicking phantom

A schematic of the fibre laser (manufactured by SPI lasers) used in the following experiments is shown in figure 1 (a). This fibre laser can provide an average power of 20W at a wavelength of 1060nm with a maximum pulse energy of 0.8mJ. The pulse repetition frequency and pulse duration could be varied from 10Hz to 390kHz and from 15 to 220ns, respectively. The pulse duration used in the following experiments was measured to be 65ns at full width half maximum. The system was compact with a height of 9cm, a width of 21cm and a length of 40cm (see figure 1 (b)) and provided a high quality beam ($M^2=1.2$).

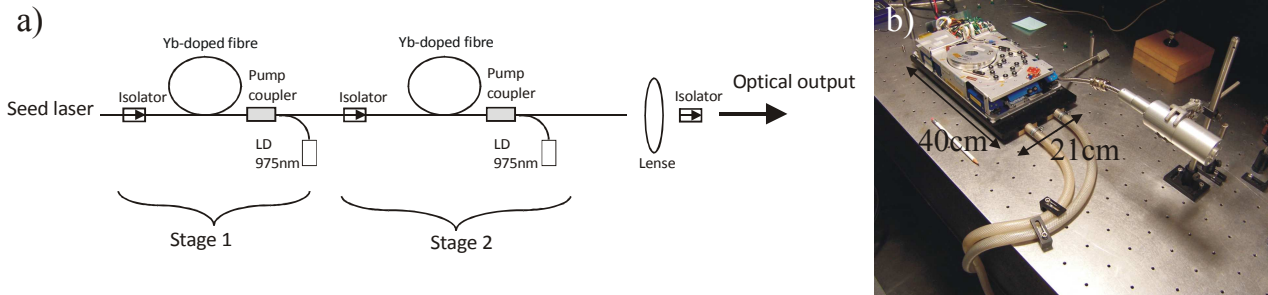


Figure 1: (a) Schematic of the fibre laser (LD: laser diode) (b) Photograph of the fibre laser.

Figure 2 (a) shows a schematic of the experimental setup used for single point measurements in a tissue mimicking phantom. The phantom is composed of three blood filled tubes of diameters 120, 250 and 580 μm placed perpendicular to the incident laser beam axis at a depth of 4.2mm, 8.6mm and 12.2mm respectively. To mimic the scattering properties of human tissue the tubes were immersed in a 1% solution of intralipid ($\mu'_s = 1\text{mm}^{-1}$). For this experiment, the fibre laser provided pulse energies of 0.5mJ at a repetition rate of 1kHz. The optical beam was expanded to approximately 8mm in diameter. The incident fluence was kept below the safe maximum permissible exposure (MPE) for skin (British Standard 1994). The photoacoustic signals were detected using a 3.5MHz cylindrical focus PZT transducer (focal length 32mm). Each signal was amplified (40dB) and signal averaged 1000 times.

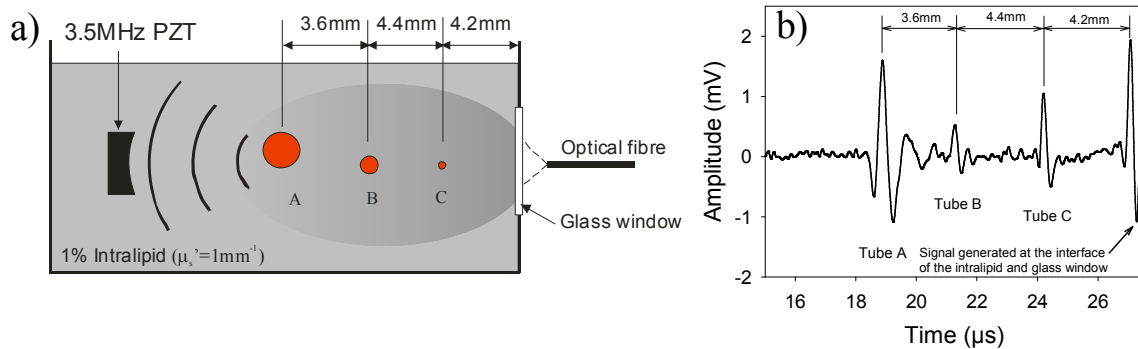


Figure 2: (a) Experimental setup, the phantom was composed of three blood filled capillary tubes (A, $\text{\O}580\mu\text{m}$; B, $\text{\O}250\mu\text{m}$; C, $\text{\O}120\mu\text{m}$) immersed in intralipid $\mu'_s = 1\text{mm}^{-1}$. (b) The detected photoacoustic signals were amplified (40dB) and signal averaged 1000 times.

Figure 2 (b) shows the detected photoacoustic signals. It can be seen that the waveform is composed of four bipolar signals. The first three bipolar signals correspond to the three blood filled tubes. The fourth bipolar signal, seen at time $t=27\mu\text{s}$, is the signal generated at the interface of the glass window and the intralipid solution. The time separation

between each of the bipolar signals, when converted to distance using the speed of sound (1480m/s), matched the measured distances between the tubes.

2.2 Photoacoustic tomography of a tissue mimicking phantom

The fibre laser was then combined with a photoacoustic imaging system to obtain 3D images. The imaging system is illustrated in figure 3 and uses an optical ultrasound sensor based upon a Fabry–Perot polymer film interferometer to detect the acoustic signals. The Fabry Perot sensor is composed of a polymer film (40µm thick) sandwiched between two dichroic soft dielectric mirrors. These mirrors are highly reflective (>95%) between 1500 and 1650nm but highly transmissive between 600nm and 1200nm. This allows the optical pulses emitted by the fibre laser (1060nm) to be transmitted through the sensor, into the underlying tissue where they are absorbed generating a photoacoustic wave. The latter then propagates back to the sensor, modulating the optical thickness of the Fabry–Perot interferometer and hence its reflectivity. The sensor is then read out by raster scanning a focussed interrogation laser beam at 1550nm over its surface and measuring the reflected light using a photodiode. From the 2D distribution of the photoacoustic waves, a 3D image is then reconstructed [9]. A more detailed description of this imaging system can be found in reference [10,11].

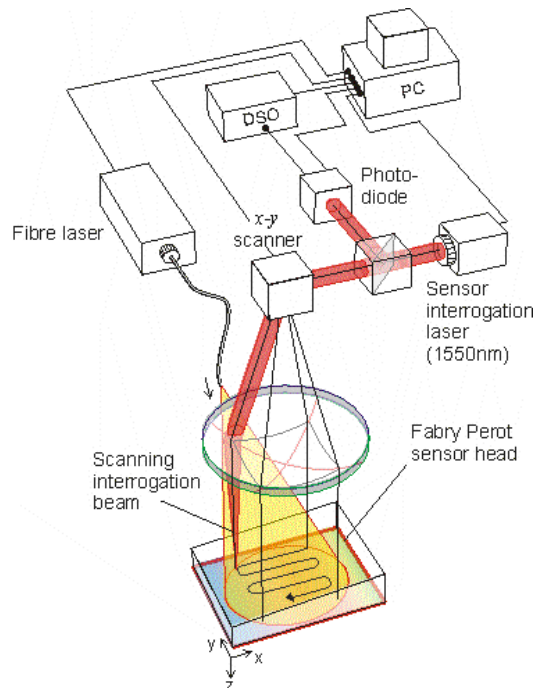


Figure 3: Photoacoustic imaging system based on a Fabry-Perot sensor.

Figure 4 (a) shows a photograph of the tissue mimicking phantom. The tissue mimicking phantom was composed of five blood filled tubes of two different diameters (250 and 580µm) placed at a range of depths (see figure 4 (a)). The tubes were immersed in a 1% solution of intralipid to mimic the scattering properties of biological tissue. The shallowest tube was placed at a depth of 1.8mm and was 250µm in diameter. The deepest tube was placed at a depth of 4mm and was 580µm in diameter. The fibre laser provided pulse energies of 0.8mJ at a repetition frequency of 100Hz for a beam diameter of 1cm. The incident fluence was below the safe MPE for skin. Photoacoustic signals were acquired over an area of 10mm x 8mm in steps of 100µm. Each signal was averaged over 100 laser pulses. Figure 4 (b) shows a maximum intensity projection of the reconstructed 3D photoacoustic image. It can be seen that all five tubes can be identified in the reconstructed photoacoustic image.

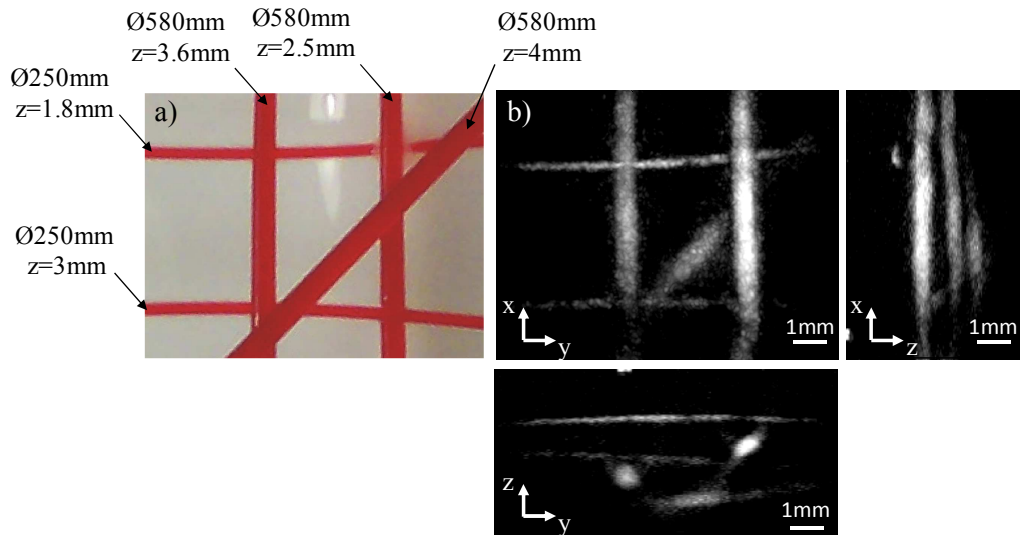


Figure 4: (a) The phantom was composed of blood filled tubes immersed in an 1% intralipid solution ($\mu'_s = 1\text{mm}^{-1}$). Each tube is located a different depth z . (b) Maximum intensity projection of the reconstructed image. Each photoacoustic signal was signal averaged 100 times.

2.3 *In vivo* photoacoustic tomography

Figure 5 (a) shows a photograph of the region of the palm which was imaged. Photoacoustic signals were acquired over an area of 9mm by 9mm in steps of $100\mu\text{m}$, each signal was low pass filtered (cut off frequency 2.5MHz) and signal averaged 16 times. The fibre laser provided pulse energies of 0.8mJ at a repetition frequency of 100Hz, for a beam diameter of 1cm. The incident fluence was kept below the safe MPE for skin. The maximum intensity projections of the reconstructed 3D image are shown in figure 5 (b). These images show the subcutaneous vasculature to a depth of approximately 2 mm. The largest vessel (labelled A) has a diameter of approximately $500\mu\text{m}$ and was located at a depth of 1.5mm. The smallest vessel (labelled B) had a diameter of approximately $150\mu\text{m}$ and was located at a depth of 1mm.

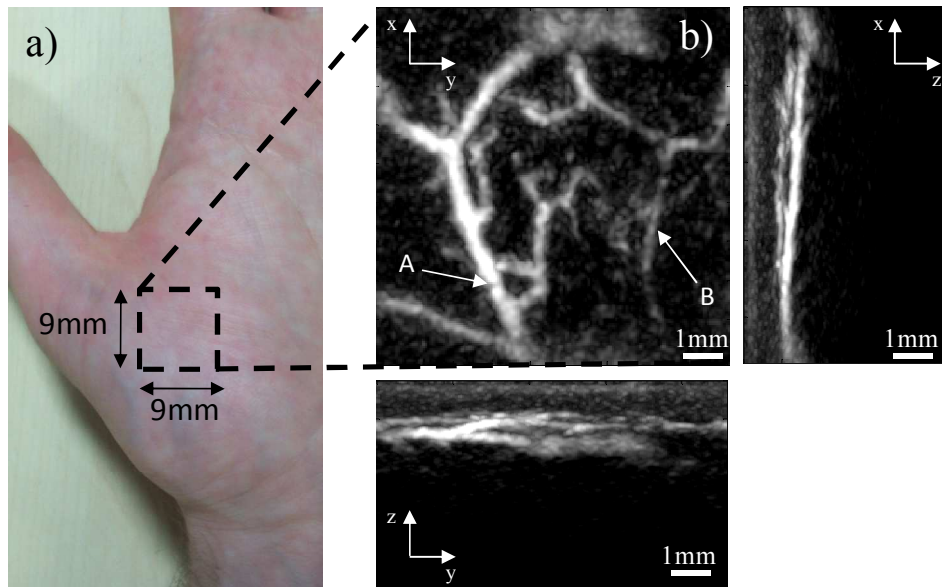


Figure 5: (a) Photograph illustrating the area of the palm that was imaged. (b) Maximum intensity projections of a 3D photoacoustic image of the vasculature of the palm of a hand. The acquired signals were signal averaged 16 times.

3. DISCUSSION & CONCLUSION

This study has shown that a pulsed fibre laser can generate photoacoustic signals both in a realistic blood vessel phantom and in vivo with sufficient SNR to achieve penetration depths of several mm when operating in tomography mode. Although in vivo images of the subcutaneous vasculature were obtained as shown in figure 5, the SNR is much lower than achieved previously with the same imaging system but using a flashlamp pumped Q-Switched Nd:YAG-OPO laser system as the excitation source [10,11]. This is in part due to the much lower pulse energy (by a factor of ~30) of the fibre laser and the non optimal wavelength of 1060nm which is absorbed significantly by water. However, there is significant scope to mitigate the low SNR. Using a larger diameter multimode fibre, pulse energies of the order of several tens of mJ should be achievable [12]. Furthermore, fibre lasers can provide high PRFs (~ten of kHz) and arbitrary control of the temporal characteristics of the laser pulse both of which can be exploited to increase SNR - the former allows rapid signal averaging to be performed and the latter provides the opportunity to downshift the acoustic frequency content of the generated photoacoustic signal in order to reduce the effects of frequency dependent acoustic attenuation in tissue [5].

The high PRF of a fibre laser also enables the acquisition speed of the imaging system to be increased thus reducing motion induced artefacts. For example, when operating at pulse energies of 0.8mJ the maximum repetition frequency the laser can provide whilst remaining below the MPE is 1250Hz for an illumination beam diameter of 1cm². This pulse repetition frequency would allow for a photoacoustic image, averaged 16 times, to be acquired four times as fast as a single photoacoustic image (not averaged) using a flashlamp pumped Q-switched Nd:YAG-OPO system operating at a typical PRF of 20Hz.

In summary, this study has demonstrated that pulsed fibre lasers have the potential to be used as an excitation source for photoacoustic tomography. Their compact size, reliability, efficiency and low maintenance makes them potentially well suited to superficial clinical imaging applications. These could include characterizing the structure and function of superficial vascular networks for the assessment of skin tumours, vascular lesions, soft tissue damage such as burns and wounds and other superficial tissue abnormalities.

4. ACKNOWLEDGEMENT

The authors would like to acknowledge SPI Lasers, the manufacturer of the fibre laser used in this study.

REFERENCES

- [1] L.V. Wang, "Tutorial on photoacoustic microscopy and computed tomography," *IEEE Journal of Selected Topics in Quantum Electronics*, vol. 14, 2008, pp. 171-179.
- [2] M. Xu and L.V. Wang, "Photoacoustic imaging in biomedicine," *Review of Scientific Instruments*, vol. 77, 2006, p. 041101.
- [3] J. Brunner and P. Beard, "Pulsed photoacoustic Doppler flowmetry using a cross correlation method," *Proceedings of SPIE*, vol. 7564, 2010, pp. 756426-756426-8.
- [4] M.P. Mienkina, C.-S. Friedrich, N.C. Gerhardt, M.F. Beckmann, M.F. Schiffner, M.R. Hofmann, and G. Schmitz, "Multispectral photoacoustic coded excitation imaging using unipolar orthogonal Golay codes," *Optics Express*, vol. 18, Apr. 2010, pp. 9076-87.
- [5] T.J. Allen, "Generating photoacoustic signals using high-peak power pulsed laser diodes," *Proceedings of SPIE*, 2005, pp. 233-242.

- [6] W. Shi, S. Kerr, I. Utkin, J. Ranasinghesagara, L. Pan, Y. Godwal, R.J. Zemp, and R. Fedosejevs, "Optical resolution photoacoustic microscopy using novel high-repetition-rate passively Q-switched microchip and fiber lasers," *Journal of Biomedical Optics*, vol. 15, 2010, p. 056017.
- [7] Y. Wang, K. Maslov, Y. Zhang, S. Hu, L. Yang, Y. Xia, J. Liu, and L.V. Wang, "Fiber-laser-based photoacoustic microscopy and melanoma cell detection," *Journal of Biomedical Optics*, vol. 16, 2011, p. 011014.
- [8] K. Maslov, H.F. Zhang, S. Hu, and L.V. Wang, "Optical-resolution photoacoustic microscopy for in vivo imaging of single capillaries.," *Optics Letters*, vol. 33, May. 2008, pp. 929-31.
- [9] K.P. Köstli and P.C. Beard, "Two-dimensional photoacoustic imaging by use of Fourier-transform image reconstruction and a detector with an anisotropic response.," *Applied Optics*, vol. 42, Apr. 2003, pp. 1899-908.
- [10] E. Zhang, J. Laufer, and P. Beard, "Backward-mode multiwavelength photoacoustic scanner using a planar Fabry-Perot polymer film ultrasound sensor for high-resolution three-dimensional imaging of biological tissues.," *Applied Optics*, vol. 47, Feb. 2008, pp. 561-77.
- [11] E.Z. Zhang, J.G. Laufer, R.B. Pedley, and P.C. Beard, "In vivo high-resolution 3D photoacoustic imaging of superficial vascular anatomy.," *Physics in Medicine and Biology*, vol. 54, Feb. 2009, pp. 1035-46.
- [12] M.Chen, Y. Chang, and A. Galvanauskas, "27 mJ nanosecond pulses in $M^2=6.5$ beam from a coiled highly multimode Yb-doped fiber amplifier" *America*, pp. 5-7.